

Inelastic Electron Scattering Study of Ni(111) Surface Phonons

W. Menezes,^a P. Knipp,^b G. Tisdale,^b and S. J. Sibener^a

The James Franck Institute, The University of Chicago
Chicago, Illinois 60637

a) Also associated with the Department of Chemistry,
The University of Chicago.

b) Also associated with the Department of Physics,
The University of Chicago.

Abstract

Inelastic electron scattering has been used to obtain the surface phonon dispersion relations for clean Ni(111) along the Γ \bar{M} symmetry direction. Kinematic conditions were varied in order to selectively examine the Rayleigh mode and “gap” mode, as well as contributions from bulk phonons. Comparison of the experimental phonon dispersion relations and inelastic scattering cross sections with lattice dynamical and quantum multiple scattering calculations demonstrate that the intraplanar surface force constant is $11 \pm 3\%$ softer than in bulk nickel, and that tensile surface stress is present at the level of 1.6 ± 0.2 N/m.

1. INTRODUCTION

In this paper we report on the surface dynamical properties of clean Ni(111) as examined by inelastic electron scattering operating at high incident energies, in the off-specular impact scattering regime. The experimental results are analyzed using both lattice dynamical and multiple-scattering calculations. Ni(111) presents an excellent opportunity for studying the dynamical properties of a closest-packed surface which has nearly ideal termination with respect to its bulk geometry. Bulk nickel dispersion curves are fit extremely well by a simple force-constant model which assumes that the interatomic potential $\phi(r)$ is only nonzero between nearest neighbors.¹ The first and second derivatives ϕ' and ϕ'' dictate the harmonic vibrations. (However, from total energy minimization, ϕ'

vanishes for this model.) Deviations of dynamical surface properties from "ideal termination" can be expressed in terms of $\phi_{ij}(r) \neq \phi(r)$, where $\phi_{ij}(r)$ is the (nearest-neighbor) potential between atoms in layers i and j . Previous studies^{2,3} indicate that the geometrical spacing between this unreconstructed surface and the second layer is within 1% of the bulk value. Hence, $\phi_{ij}(r) - \phi(r)$ is expected to be small.

2. EXPERIMENTAL

Our surface phonon measurements were carried out in a new electron scattering instrument which uses 127° cylindrical deflection optics. It consists of a fixed geometry double pass monochromator and a rotating single pass analyzer.⁴ The analyzer rotates in the scattering plane, covering the angular range 82°-137° with respect to the monochromator. The scattering plane includes the surface normal. The instrumental resolution was 5-6 meV over the entire (1-250 eV) range. The in-plane angular width of the specular low energy electron diffraction (LEED) beam, as measured with the rotating HREELS analyzer, was 1.5°. This width contains contributions from both the finite domain size of the surface and the instrument transfer function of the electron spectrometer. It corresponds to a momentum transfer resolution of $\pm 0.04 \text{ \AA}^{-1}$ for typical experimental configurations. The detector angle could be reproducibly positioned to within 0.1°.

The Ni(111) single crystal was polished to 0.05 μm and cut to within 0.5° of the desired orientation. This was confirmed using Laue x-ray backreflection. The $\Gamma\bar{M}$ azimuthal orientation was selected by rotating the crystal until the $(0\bar{1})$ diffraction rod was detected with the HREELS analyzer. LEED I-V profiles established the absolute azimuthal orientation of the crystal. The crystal was cleaned by cycles of Ar^+ bombardment followed by annealing at 1000 K. Auger analysis verified surface cleanliness, while sharp LEED beams and low diffuse elastic scattering indicated the success of our annealing procedure. Crystal temperature was monitored with a type K thermocouple that was spot welded to the side of the crystal. The base pressure in the crystal chamber was typically 5×10^{-11} Torr during data acquisition. Liquid nitrogen cooling of the target mount permitted data collection with surface temperatures as low as $T_s = 110 \text{ K}$.

3. RESULTS

We have observed the Rayleigh mode (S_1), “gap” mode (S_2), and contributions from bulk modes, i.e. surface resonances, (R_1) at several points along the $\Gamma\bar{M}$ azimuth. Near $\bar{Q} = \bar{M}$, S_1 and S_2 are primarily localized in the surface layer and polarized shear vertically (SV) and longitudinally, respectively. The electron-phonon scattering cross-sections depend non-monotonically on the scattering geometry and incident beam energy. Thus by choosing the appropriate scattering parameters, several surface phonon modes can be individually resolved. In order to optimize the scattering cross sections for various surface phonon modes, and to find energetic windows where individual modes could be resolved, many survey spectra were recorded with various angles of incidence and beam energies at the \bar{M} point in the SBZ.

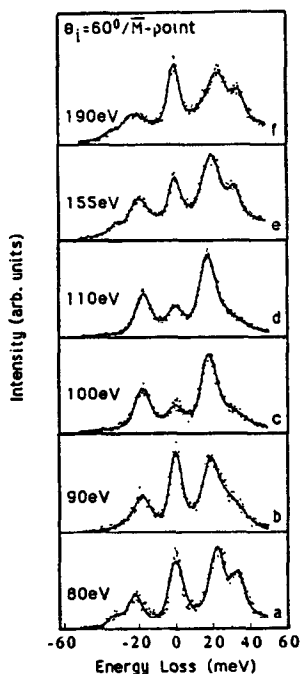


Figure 1. Series of energy loss spectra recorded at different impact energies. Incident polar angle was fixed at 60° , while final angle was adjusted to probe the \bar{M} point ($Q_{\parallel} = 1.46 \text{ \AA}^{-1}$) of the surface Brillouin zone. All panels have linear Y axis, scaled from: (a), (e) and (f), 0.0 to 1.0; (b), 0.0 to 2.0; (c), 0.0 to 2.5; (d), 0.0 to 3.0.

Figure 1 illustrates a few examples recorded at fixed incident angle $\theta_1=60^\circ$. At each beam energy the Γ point was accessed by rotating the analyzer to the appropriate final angle. Several narrow (a, d) and broad (e, f) features are seen in these spectra. The peaks at ± 17.3 meV in figure 1d corresponds to the creation and annihilation of the S_1 phonon. Its dispersion along the Γ \bar{M} direction was mapped by keeping the incident kinematics fixed ($E_1=110$ eV and $\theta_1=60^\circ$) and varying the analyzer angle (θ_5) to generate the appropriate value for the parallel momentum transfer ($Q_{||}$). These measurements were primarily made in the second SBZ towards the surface normal, since the intensities were approximately 2 to 3 times higher than in the first SBZ.

Scattering conditions were also found which allowed us to examine the S_2 and R_1 modes. The S_2 dispersion in the gap has been mapped using $E_1 \approx 155$ eV and $\theta_1 = 60$. Spectral density plots show a large R_1 intensity originating in the second layer with Z polarization.

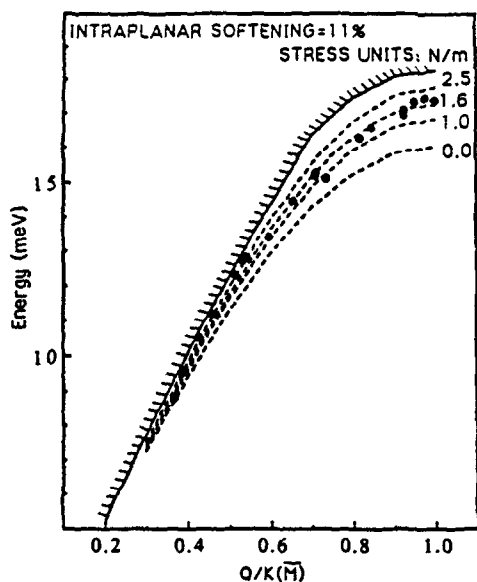


Figure 2. Expanded view of the S_1 surface phonon dispersion along the Γ \bar{M} direction illustrating the sensitivity of the lattice dynamical fits to various levels of surface stress.

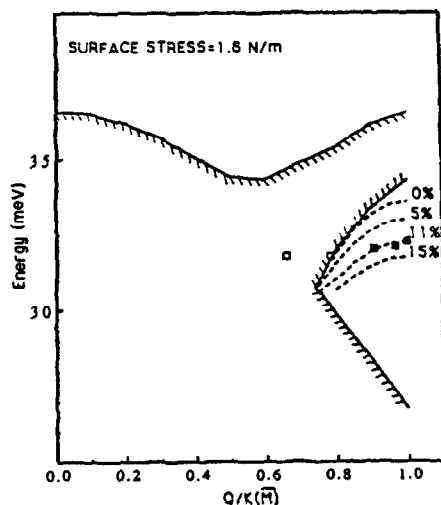


Figure 3. Expanded view of the S_2 surface phonon dispersion along the Γ \bar{M} direction illustrating the sensitivity of the lattice dynamical fits to the extent of intraplanar force constant softening

Figures 2 and 3 show the experimental dispersion relations and lattice dynamical calculations for the Ni(111) surface phonons plotted as a function of the reduced parallel momentum transfer $\zeta \equiv Q/K(\bar{M})$, where $K(\bar{M}) = 1.457 \text{ \AA}^{-1}$. The data points for S_1 lie *higher* in energy than expected from the dispersion relation generated by a Green's function calculation⁵ which assumes that the surface force constants are unchanged from the bulk value. Such a "surface phonon anomaly" requires the use of modified surface force constants (specifically ϕ''_{12} and/or ϕ'_{11}) to reconcile experiment and theory. However, arguments based on Badger's rule,⁶ which correlates bond length variation [$\leq 1\%$ for Ni(111)] and force constant change, discourage sizable modification in ϕ''_{12} to fit our data for S_1 . Instead, we get a good fit by assuming a tensile (attractive) surface stress with $\phi'_{11}/r = +(1.6 \pm 0.2) \text{ N/m}$, where $r = 2.49 \text{ \AA}$ is the Ni-Ni distance. For comparison, Table I lists the surface stresses for Ni(111), Ni(100) and Ni(110), all of which should be compared to the bulk nickel force constant $\phi'' = 37.6 \text{ N/m}$. A correlation is evident between surface stress and the packing density of the topmost layer.

Table I.
Nickel surface stresses

Miller index	Direction	Surface Packing Density (r^{-2})	ϕ'/r ^(a) (N/m)	Reference
(111)	$[\bar{1}\bar{1}0]$	1.155	+1.6±0.2	This work
(001)	$[\bar{1}\bar{1}0]$	1.000	+1.9	Ref. 7
(110)	$[\bar{1}\bar{1}0]$	0.707	+3.0	Ref. 7
(110)	[001]	0.707	+4.2	Ref. 7

(a) For comparison, the bulk nickel force constant $\phi'' = 37.6 \text{ N/m}$.

Contrary to the S_1 findings, the data for S_2 lie *lower* in energy than the dispersion relation generated with the simple lattice dynamical model, Figure 3. The best agreement between the theoretical and experimental

dispersion curves for S_2 is attained when ϕ''_{11} is softened by $11 \pm 3\%$. This modest amount of intraplanar softening is reminiscent of the electron scattering Cu(111) results.⁸

One should also note that previous helium scattering experiments on the (111) surfaces of copper,⁹ silver,^{9,10} and platinum¹¹ indicated 50%, 50%, and 40% softenings, respectively, of the intraplanar surface force constant ϕ''_{11} . However, these studies could not probe S_2 . Owing to its longitudinal polarization, S_2 is very sensitive to ϕ''_{11} . The Cu(111) HREELS experiments⁸, which also probed S_2 , demonstrated surface phonon characteristics which required only 15% softening, consistent with a recent "embedded atom method" calculation.¹² Owing to its SV polarization, S_1 is sensitive to both the interplanar force constant ϕ''_{12} and the surface stress ϕ'_{11} (from equilibrium considerations, ϕ'_{12} vanishes). This has been demonstrated for Ni(100),¹³ Ni(110),⁷ and Cu(100).¹⁴ Only in the case of Ni(110) was the existence of surface stress unambiguous.

One might contest that the single force constant model used here is too simplistic, thereby invalidating our results. Black *et al.*¹⁵ calculated the surface phonons for Ni(111), using a sizable assortment of interatomic potentials fitted to neutron scattering data and assumed to persist unchanged near the surface. For each model used, $S_1(\bar{M}) < 16.2$ meV and $S_2(\bar{M}) > 33.1$ meV. Since our values (17.2 ± 0.3 meV and 32.2 ± 0.3 meV) fall well outside of these limits, the effects of surface force field relaxation are unambiguous.

To confirm our spectroscopic findings, we have also performed quantum scattering calculations. The rigid-ion multiple-scattering (RIMS) method¹⁶ generated inelastic matrix elements which were combined¹⁷ with vibrational spectral densities to yield the (unnormalized) single phonon cross section. To this were added a delta function in the elastic channel to simulate the diffuse scattering from defects and impurities, and a two-parameter Gaussian in order to approximate multiphonon contributions. The total was convoluted with the instrument transfer function to compare directly with experiment. Figures 4(a) and 4(b) show such fits to the data, yielding best fit parameters of 1.6 N/m and 11% for the surface stress and intraplanar softening, respectively, in agreement with our (independent) spectroscopic conclusions.

In addition to scattering from true surface modes such as S_1 and S_2 , HREELS measurements can also contain contributions from bulk phonons.¹⁸ In the top layer of the crystal, bulk and surface phonons contribute to the

vibrational spectral density in roughly equal amounts. Deeper inside the crystal, bulk modes dominate the vibrational behavior. Because electrons can penetrate a few layers into the bulk before being inelastically scattered, their interactions can accordingly be dominated by bulk phonons under suitable conditions. Figure 4(c) shows a spectrum taken with $E_i = 100$ eV, $\theta_i = 70.0^\circ$, and $\zeta = \bar{M}$ which has intense energy loss and gain features centered around 23 meV. These peaks reside in the bulk band, so cannot be attributed to surface phonons. The R_1 scattering was intense only in a small angular range around \bar{M} .¹⁹ This R_1 dispersion behavior bears remarkable similarity to recent embedded atom method calculations for Cu(111), as shown in Figure 6a of ref.¹². This abrupt appearance of R_1 differs from the behavior of the "longitudinal resonance" (LR) discussed in previous studies,⁸⁻¹² which was seen to disperse across the surface Brillouin zone, approaching zero linearly at \bar{T} . Our attempts to fit quantitatively the scattering data for R_1 were poor; therefore, we have not attempted to extract surface information from it.

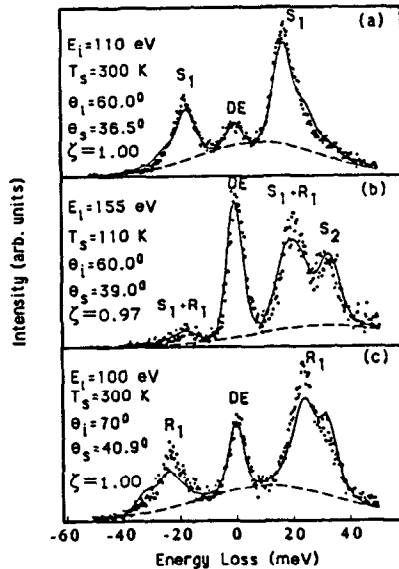


Figure 4. Experimental spectra and quantum scattering calculations for kinematic conditions which optimized sensitivity to (a) S_1 , (b) S_2 , and (c) R_1 . The dashed line in each panel represents the estimated multiphonon contribution. Surface force constant model: 11% intraplanar softening and 1.6 N/m tensile surface stress.

4. SUMMARY

To summarize, these results demonstrate that the surface force field for Ni(111) differs from expectations based upon simple extrapolation from bulk behavior. The intraplanar surface force constant is approximately 11% softer than in bulk nickel. In addition, tensile surface stress is present at the level of +1.6 N/m, indicating that the surface atoms have a desire to be more closely spaced than in the bulk. This level of stress has been predicted theoretically for a number of metal surfaces.²⁰ These surface force field assignments were derived from lattice dynamical fits to the spectroscopic results, and were independently confirmed by multiple scattering calculations. Such calculations show that the scattering peaks are sensitive to the lattice dynamical model used, both in position and intensity. By varying the experimental parameters, we were able to resolve the different phonon features as desired. It is hoped that the precision surface phonon measurements that are now available for Ni(111) will stimulate improved *ab initio* calculations on this interface.

5. ACKNOWLEDGEMENTS

We are extremely grateful to Helmut Krebs and the University of Chicago Machine Shop for their technical assistance. We wish to thank Ugo Fano for stimulating discussions. We also wish to thank Burl Hall and Doug Mills for their scattering computer code and for numerous helpful conversations. This work was supported, in part, by the Air Force Office of Scientific Research, the Department of Defense University Research Instrumentation Program; and the National Science Foundation Materials Research Laboratory at the University of Chicago.

References

1. R.J. Birgeneau, J. Cordes, G. Dolling, and A.D.B. Woods, *Phys. Rev.* **136**, A1359 (1964)
2. T. Narusawa, W.M. Gibson, and E. Törnqvist, *Surf. Sci.* **114**, 331 (1982).
3. J.E. Demuth, P.M. Marcus, and D.W. Jepsen, *Phys. Rev. B* **11**, 1460 (1975).
4. Electron optics fabricated by LK Industries, modified to allow analyzer rotation.
5. J.E. Black, Talat S. Rahman, and D.L. Mills, *Phys. Rev. B* **27**, 4072 (1983).
6. Richard M. Badger, *J. Chem. Phys.* **2**, 128 (1943).
7. S. Lehwald, F. Wolf, H. Ibach, Burl M. Hall, and D.L. Mills, *Surf. Sci.* **192**, 131 (1987).
8. Mohamed H. Mohamed, L.L. Kesmodel, Burl M. Hall, and D.L. Mills, *Phys. Rev. B* **37**, 2763 (1988); Burl M. Hall, D. L. Mills, Mohamed H. Mohamed, and L. L. Kesmodel, *ibid.* **38**, 5856 (1988).
9. U. Harten, J.P. Toennies, and Ch. Wöll, *Faraday Discuss. Chem. Soc.* **80**, 137 (1985).
10. Bortolani, A. Franchini, F. Nizzoli, and G. Santoro, *Phys. Rev. Lett.* **52**, 429 (1984).
11. K. Kern, R. David, R.L. Palmer, G. Comsa, and T.S. Rahman, *Phys. Rev. B* **33**, 4334 (1986).
12. J.S. Nelson, M.S. Daw, and Erik C. Sowa, *Phys. Rev. B* **40**, 1465 (1989). There are numerous typographical errors in Table I of this reference.
13. S. Lehwald, J.M. Szeftel, H. Ibach, T.S. Rahman, and D.L. Mills, *Phys. Rev. Lett.* **50**, 518 (1983).
14. M. Wuttig, R. Franchy, and H. Ibach, *Z. Phys. B* **65**, 71 (1986).
15. John E. Black and R.F. Wallis, *Phys. Rev. B* **29**, 6972 (1984); J. E. Black, F. Shanes, and R. F. Wallis, *Surf. Sci.* **133**, 199 (1983).
16. Mu-Liang Xu, B.M. Hall, S.Y. Tong, M. Rocca, H. Ibach, and S. Lehwald, *Phys. Rev. Lett.* **54**, 1171 (1985).
17. P. Knipp and Burl M. Hall, *Surf. Sci.* (accepted).
18. M. Rocca, S. Lehwald, H. Ibach, and Talat S. Rahman, *Surf. Sci.* **171**, 632 (1986).
19. W. Menezes, P. Knipp, G. Tisdale, and S. J. Sibener, *Phys. Rev. B* **41**, 5648 (1990).
20. M.C. Payne, N. Roberts, R.J. Needs, M. Needels, and J.D. Joannopoulos, *Surf. Sci.* **211/212**, 1 (1989).